Impedance-based Higher Order Sliding Mode Control for Grasping and Manipulation

Rakibul Hasan, Ranjan Vepa, Hasan Shaheed

School of Engineering and Materials Science
Queen Mary, University of London, London, UK
{m.r.hasan,r.vepa,m.h.shaheed}@qmul.ac.uk

Abstract—Grasping and manipulation by multifingered robot hand is challenging due to the dynamic uncertainties of the hand and the object. The purpose of the grasping and manipulation research is to improve the control performance based on the hand, object and contact model. In this paper, a multifingered hand called The Barrett Hand is chosen for investigation. A mathematical model of the hand is developed using Lagrangian method. Contact model between the hand and object is developed as compliance system assuming that the object stiffness properties are known. Grasping and manipulation control problem is stated as: 1. Object motion and 2. Contact force tracking. Higher Order Sliding Mode (HOSM) control is proposed for motion tracking of the hand joints and object. 2nd order sliding mode law is used to minimise the tracking error considering nonlinear dynamics and uncertainties. Adaptive Force-based Impedance Mode (AFIM) control is proposed to regulate the contact force which drives the desired impedance of the hand-object compliance system. This impedance also generates online reference trajectory for motion tracking according to the contact force. Both control methods are simulated in Simulink/SimMechanics environment. The joint, object and force tracking results are presented and discussed.

Keywords–Grasping; Sliding; Impedance; Adaptive; AFIM; HOSM.

I. INTRODUCTION

Conventional robot manipulators used in industries are combined form of single arm attached to a gripper. The gripper is effective in performing tasks where the large motion of the payload required with fewer Degrees of Freedom (DOF). Traditional grippers are unable to show the efficiency where precise movement is needed for the object manipulation [2]. Grippers are being replaced now by the human hand alike multifingered hand to ease the grasping and manipulation activities by industrial manipulators.

Human hand grasps and manipulates an object by several steps: 1. The human eye works as sensor to locate the object location. 2. Hand moves to the object location with previous grasp planning knowledge. 3. When grasp is planned, fingers make contact with assumed forces, but change the force depending on the object's mass, stiffness and material properties. These properties are sensed by the brain to send the signals to the arm and hand to apply the optimized forces for grasping and manipulation of the object. The above procedures are not simple in robot hand grasping and manipulation. In an attempt to attain the identical abilities of the human hand, research has been going on for last two decades. In the early stage of the grasping research, Okada discussed the computer control method of multijoint finger system for precise object handling [11]. Mason and Salisbury formulated the grasp problem and introduced the grasp jacobian [10]. Kerr and

Roth worked on grasp kinematics [8]. Bicchi and Okamura focused on grasping and manipulation of unknown objects [2][12]. Currently, several multifingered hands are available in the industries and also for the research. The robot hand is a complex system due to the presence of additional DOF for dexterity. In addition, this is not similar to the custom gripper which is efficient in generating a specific rigid grasp of an object. The same grasp with multifingered hand requires intelligent control and results in a decrease in grasp rigidity.

In this paper, two advanced robust control methods are applied for grasping and manipulation of an object by a robot hand. Higher Order Sliding Mode (HOSM) is implemented for position accuracy of the robot containing uncertainties and Adaptive Force based Impedance Method (AFIM) is applied to minimize the contact forces during manipulation. Both methods are advanced and powerful in achieving position and force control respectively in individual robotic tasks. Therefore, those are applied together in grasping and manipulation of the hand which is related to combined position and force problem. To implement and see the performances, a three fingered robot hand is modeled, contact model between the hand and the object is derived, control problem of grasping and manipulation is defined and robust adaptive controllers are designed according to the problem requirements. Contact locations and types are assumed to be known for simplifying grasp planning. The other assumptions made in studying the kinematics are that the fingers do not slip on the object, the object and finger links are rigid body, accurate models of the hand and object are known.

In next four subsections, grasp properties, robot and object kinematics and dynamics are derived. Section 2 explains the control theories behind HOSM and AFIM. The control laws implemented for the robot hand are also included here. Simulation of the proposed control and the results are presented in Section 3. The last section provided the summary of the work and future aspects.

A. Grasp and manipulation properties

A grasp is defined as a combination of hand posture and position that generates a contact force set between the hand and the grasped object. The grasp jacobian maps the relation between the object and the hand through this contact force. It is first proposed by Mason and Salisbury [10]. The popular Barrett hand is considered for analysing grasping and manipulation properties in this paper. It is used in industries for different tasks and available for research activities. Consider this three fingered hand grasping an object in Figure 1 [15]. Each finger has two DOF available for the grasping and manipulation tasks. Lets define the object coordinate frame
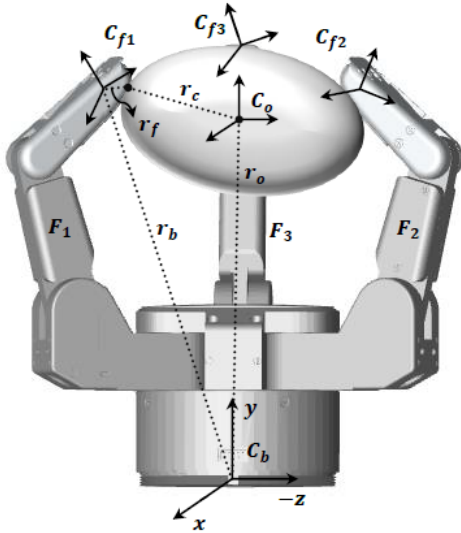
Figure 1. The Barrett Hand model grasping an object [15].

as C_o where center of mass of the object is chosen as the object reference point. C_b is the palm frame and $C_{f,i}$ is the contact coordinate (i= contact number). The term $r_o = [p_o, o_o]$ is the position vector of the origin of C_o with respect to C_b where p_o is the position and o_o is the orientation vector of the object origin. The term $r_b = f(q_i)$ is the position vector of the origin of $C_{f,i}$ with respect to C_b. The term r_c is the position vector from the origin of C_o to contact coordinate $C_{f,i}$ with respect to C_b. All contacts between the object and hand are considered as point contact without slip. If each finger applies a force $f_{c,i}$ at the contact point $C_{f,i}$, the applied object wrench is given as,

$$\sum_{i=1}^{n} G_i F_{c,i} \tag{1}$$

where, $F_o = [f_o^T \quad m_o^T]^T$ is the external force exerted on the object and $G_i \in \Re^{6 \times n}$ is called the grasp Jacobian matrix which transforms the contact force $f_{c,i}$ to the object coordinate frame (n is the number of contacts) and is given by,

$$G_i = \begin{bmatrix} I_3 \\ r_c \times \end{bmatrix} \tag{2}$$

where, I_3 is the 3×3 identity matrix and $[r_c \times] \in \Re^{3 \times 3}$ is a skew symmetric matrix determined by the cross product of r_c. The full grasp matrix can be shown as $G = [\ G_1 \quad G_2 \quad \dots \quad G_n\ ]$ and the contact force set, $f_c = [\ f_{c1}^T \quad f_{c2}^T \quad \dots \quad f_{cn}^T]^T$. The contact force $f_{c,i} \in FC$ where, $FC = \{f \in \Re^3 \left\{ f \in \Re^3 : \sqrt{f_1^2 + f_2^2} \leq \mu f_3 \right\}$ is called the friction cone, which is the angle of the cone with respect to contact normal [10][13]. Similarly, the matrix which transforms the contact force $f_{c,i}$ to the finger coordinate frame is given by,

$$F_i = A_i f_{c,i} \tag{3}$$

where, $A_i \in \Re^{6 \times n}$ and have the following matrix form,

$$A_i = \begin{bmatrix} I_3 \\ r_f \times \end{bmatrix} \tag{4}$$

the term, $[r_f \times] \in \Re^{3 \times 3}$ is the cross product of r_f. Now, if the i-th finger of the hand manipulates an object; the velocity relation $\dot{r}_{o,i} = \dot{r}_{f,i}$ is valid where, $\dot{r}_{o,i}$ is the object and $\dot{r}_{f,i}$ is the fingertip velocity at i-th contact point and both are equal, assuming there is no slip during contact. Considering the transformation with respect to base frame, the velocity relation can be expressed as,

$$G_i^T \dot{x}_o = J_{hi} \dot{q}_i \tag{5}$$

Equation (5) is the fundamental grasp constraint which governs the grasp and manipulation of an object by contact force related to the hand and the object velocity. The term $\dot{x}_o = \begin{bmatrix} \dot{r}_o^T & \omega_o^T \end{bmatrix}^T$ is the velocity vectors of the object and ω_o is the angular velocity of the object with respect to the base frame C_b. Now define the jacobian form in the finger space as, $J_{hi} \in \Re^{6 \times l} = A_i^T J_i$ as the kinematic jacobian at the i-th finger; where l_i are the number of links for fingers and J_i is the kinematics jacobian of the i-th finger. The orientation vector, $\zeta = [\ \phi \quad \theta \quad \psi\ ]^T$ of the object is represented by Z-Y-Z Euler angles. Based on Euler transformation, the relation between object velocity $\dot{x}_o$ and $\dot{r}_o$ can be shown as,

$$\dot{x}_o = T_o(\xi) \dot{r}_o \tag{6}$$

where, $T_o(\xi) \in \Re^{6 \times 6}$ is a transformation matrix between two velocity vectors given as,

$$T_o(\zeta) = \begin{bmatrix} I_3 & 0 \\ 0 & \prod(\xi) \end{bmatrix} \tag{7}$$

and $\prod(\xi)$ is represented by the following transformation matrix,

$$\prod(\xi) = \begin{bmatrix} -\sin\theta\cos\psi & \sin\psi & 0 \\ \sin\theta\sin\psi & \cos\psi & 0 \\ \cos\theta & 0 & 1 \end{bmatrix} \tag{8}$$

B. Object dynamics

Using (8) - (10), the object dynamics can be expressed by Newton-Euler equation in following form:

$$\begin{bmatrix} m_o I & 0 \\ 0 & I_b \end{bmatrix} \begin{bmatrix} \ddot{x}_o \\ \dot{\omega}_o \end{bmatrix} + \begin{bmatrix} 0 \\ \omega_o \times I_b \omega_o \end{bmatrix} = \begin{bmatrix} f_o \\ \tau_o \end{bmatrix} \tag{9}$$

where, m_o is the mass of the object and $I_b = \Pi(\xi)$. Let X_o be the local parametrization of x_o to transform (9) in local coordinate as,

$$M_o \ddot{X} + C_o(X, \dot{X})\dot{X} = F_o \tag{10}$$

where, $M_o \in \Re^{6 \times 6}$ is the object mass matrix, and the object coriolis terms are expressed as $C_o(X, \dot{X})$. The resultant force exerted on the object is $F_o = [f_o^T \quad \tau_o^T]^T$. Now, applying (1), (10) is rearranged as,

$$M_o \ddot{X} + C_o(X, \dot{X})\dot{X} = GF_c + f_e \tag{11}$$

Equation (11) is the object dynamics where contact force F_c is related to the object motion and f_e occurs due to external forces. Recall (5) and rewrite as follows:

$$\dot{q} = (A^T J)^{-1} G^T \dot{X}_o \tag{12}$$

Differentiating (12) yields,

$$\ddot{q} = (A^T J)^{-1} G^T \ddot{X}_o + \frac{d}{dt}((A^T J)^{-1} G^T)\dot{X}_o \tag{13}$$

where, $\ddot{q}$ is the joint acceleration related to the object motion.

1) Robot hand Kinematics and Dynamics: The robot hand dynamics is derived from the hand kinematics. According to the Figure 1, the Barrett hand has 3 fingers, each finger has 2 links. All fingers are identical in shape and dimension, but finger F_1 and F_2 have extra DOF. Let $(x, y, z)_{F,i}$ be the coordinates of the fingers and the forward kinematics of the fingers F_i $(i = 1, 2)$ are,

$$x_{F,i} = (l_1 \cos(q_1 + q_{i_1}) + l_2 \cos(q_1 + q_2 + q_{i_1} + q_{i_2})) \sin(\phi)$$
$$y_{F,i} = l_1 \sin(q_1 + q_{i_1}) + l_2 \sin(q_1 + q_2 + q_{i_1} + q_{i_2})$$
$$z_{F,i} = (l_1 \cos(q_1 + q_{i_1}) + l_2 \cos(q_1 + q_2 + q_{i_1} + q_{i_2})) \cos(\phi)$$
$$\tag{14}$$

and the forward kinematics of the finger F_3 are,

$$y_{F,3} = l_1 \sin(q_1 + q_{i_1}) + l_2 \sin(q_1 + q_2 + q_{i_1} + q_{i_2})$$
$$z_{F,3} = (l_1 \cos(q_1 + q_{i_1}) + l_2 \cos(q_1 + q_2 + q_{i_1} + q_{i_2}))$$
$$\tag{15}$$

where, $q_{i1} = 2.46°$ and $q_{i2} = 40°$. For Cartesian coordinate position (x_c, y_c, z_c), the joint angles of the fingers can be calculated with inverse kinematics using simple algebra and trigonometry [10].

Robot dynamics is determined by the Lagrangian method. The Lagrangian L is determined as the difference of kinetic (T) and potential (V) energy of the system [10][16]. Now, differentiate the Lagrangian L to derive the equations of motion of the system from the following term,

$$T_i = \frac{\partial}{\partial t}\left(\frac{\partial L}{\partial \dot{q}_i}\right) - \frac{\partial L}{\partial q_i} \tag{16}$$

where, i=1,2,3.....n is considered as DOF of the system. Robot finger dynamics are derived using (16) as,

$$M_{f_i}\ddot{q} + C_{f_i}(q, \dot{q})\dot{q} + N_{f_i}(q) = \tau_{f_i} \tag{17}$$

where, $M_{f_i} \in \Re^{3\times3}$ is the hand mass matrix, $C_{f_i}(q, \dot{q}) \in \Re^{3\times3}$ is the vector of the coriolis and centrifugal terms and $N_{f_i} \in \Re^{3\times1}$ are the gravity terms for the fingers F_1 and F_2. For the finger F_3, $M_{f_3} \in \Re^{2\times2}, C_{f_3}(q, \dot{q}) \in \Re^{2\times2}$ and $N_{f_3} \in \Re^{2\times1}$. The finger joint acceleration $\ddot{q}$ is calculated from (17) as,

$$\ddot{q} = M_f^{-1}(\tau_f - C_f(q, \dot{q}) - N_f(q)) \tag{18}$$

Substitute, (18) into (13), the robot-object dynamics at object frame is written in the following form,

$$M_{of}\ddot{q} + C_{of}(q, \dot{q}) + G_{of}(q) = \tau_{OF} \tag{19}$$

where, M_{of}, C_{of} and G_{of} are combined robot-object terms and have the following expression after rearranging,

$$M_{of} = M_o + GJ_h^{-T}M_f(q)J_h^{-1}G^T$$
$$C_{of} = C_o + GJ_h^{-T}\left(C_f(q, \dot{q})J_h^{-1}G^T + M_f(q)\right)\frac{d}{dt}(J_h^{-1}G^T)$$
$$G_{of} = GJ_h^{-T}N_f(q)$$
$$\tag{20}$$

2) Grasp Problem: Control problems of grasping and manipulation by a robot hand is defined following (19) as,

Object Tracking: Given a desired object trajectory $X_{do} \in \Re^6$ the center of mass of the object $X_o \in \Re^6$ should track it while the object is grasped by three fingered robot hand considering grasp constraint. The first control objective is,

$$\lim_{t\to\infty} X_{do} - X_o = 0 \tag{21}$$

Contact Force Tracking: Given a desired contact force $F_d \in \Re^9$ the actual force $F_c \in \Re^9$ should follow the desired force. The second objective is,

$$\lim_{t\to\infty} F_d - F_c = 0 \tag{22}$$

Object tracking problem is also associated with the robot finger tracking problem. Robot fingers are tracked for desired contact location before the object is grasped. Following the properties of the friction cone, it can be shown that for an arbitrary set of contact force F_c, an internal force F_I is found such that $F_c + F_I$ lies in the friction cone. This internal force does not have any net effect on the motion of the hand or object.

II. CONTROLLER DESIGN

Different control methods are available for solving the control problem defined above. Classical and adaptive sliding based controllers were used in the past for object tracking solution [1][16]. Recently Higher Order Sliding Methods (HOSM) showed robustness for perfect tracking considering uncertainties [4][5]. For force tracking problem, impedance controllers by Hogan have been used in robotics for last two decades [6]. Based on Hogan, Seraji and Jungs work, Adaptive Force based Impedance Method (AFIM) is used for force tracking [6][7][13]. In this paper, the HOSM is used for tracking control. The AFIM is used for optimizing the contact force. The control solution will be divided into three steps:

1. Given a desired contact location, HOSM is used for tracking the current position of the finger before grasp. 2. Considering grasp constraint, AFIM is implemented to optimize the contact force 3. The object trajectory is tracked with HOSM based on the contact force.

A. Higher Order Sliding Mode Control (HOSM)

The robot hand contains dynamic nonlinearities and uncertainties. Joint tracking is not simple considering uncertain dynamics due to unmodeled mechanics, external disturbances etc. The controller robustness is important to overcome this dynamic uncertainties and achieve good tracking. HOSM is a robust controller, which deals greatly with disturbances and uncertainties. It is an extended version of Sliding Mode control (SMC) [9]. Lets introduce SMC applied by a sliding surface with high frequency switching control. The goal of SMC is to converge the actual system to the desired state. In general, SMC has chattering problem due to the discontinuous nature of control. It excites unexpected high frequency dynamics which may cause damage to the system. HOSM is effective in reducing chattering problem that also guarantees the convergence of system state in finite time. In this method, the sliding variable is extended to accelerate the system state towards the selected sliding surface. Considering the tracking control problem, the general SMC is defined as,

$$s(q, t) = \dot{e} + \lambda e \tag{23}$$

where, $e_q = q - q_d$ is the finger tracking error and $e_o = X_o - X_d$ is the object tracking error and λ is a constant whose eigenvalues are always positive. The control goal is achieved

by choosing the control input such that the sliding surface fulfills the following condition:

$$\frac{1}{2}\frac{d}{dt}s^2 \leq \eta\,|s| \tag{24}$$

where, η is a positive constant. The above condition states that the system energy decays until the system state reaches the sliding surface. In HOSM, the discontinuous control input is applied to a higher time derivative of the sliding surface. The applications of HOSM in non-linear systems are found in [4][5]. Levant proposed a method of arbitrary order sliding mode controller design is discussed [9]. Defoort developed a robust HOSM controller for finite time stability [4]. For specifying HOSM, consider the non-linear system as,

$$\begin{matrix}\dot{x} = f(x,t) + g(x,t) \\ y = s(x,t)\end{matrix} \tag{25}$$

The relative degree r of system (24) is assumed to be known with respect to the sliding variable s. The control goal is to reach s=0 in finite time and hold by discontinuous function of s and its derivatives $s, \dot{s}, \ddot{s}\cdots\cdots\cdots s^{r-1}$. The r-th order sliding mode is expressed as,

$$S^r = \{u \parallel s, \dot{s}, \ddot{s}\cdots\cdots\cdots s^{r-1} = 0\} \tag{26}$$

The mode $s = 0$ is achieved after finite time transient. The control input appears at the *r-th* order sliding set as,

$$S^r = h(x,t) + g(x,t) \tag{27}$$

where $h(x,t) = s^r|_{u=0}$, $g(x,t) = \frac{\partial}{\partial u}s^r \neq 0$. From HOSM structure of (26) and (27), the controller u_h is chosen as,

$$u_h = \alpha sign\left(\frac{\dot{s}_h + \sqrt{|\,s_h\,|}sign(s_h)}{\dot{s}_h + \sqrt{|\,s_h\,|}}\right) \tag{28}$$

where, $h = f/o$, (f for finger and o for object). Equation (28) is the HOSM law proposed for finger and object tracking. The sliding variable s_h is expressed from tracking error e_q and e_o as,

$$s_h = \dot{e}_h + \lambda_h e_h \tag{29}$$

The control input torque for trajectory tracking is expressed as a combination of SMC and HOSM below,

$$u_{hosm} = u_c + u_h \tag{30}$$

where, input u_c is expressed as,

$$u_c = \bar{u} - Ks_c = M\ddot{q}_r + C\dot{q}_r + G - Ks_c \tag{31}$$

The term K is the sliding gain and the sliding function s_c is considered from (23).

B. Adaptive Force based Impedance Control

For grasping and manipulation, the important task is to maintain the contact force when the object is grasped. Position and force cannot be maintained at the same time, but the contact force can be regulated by controlling the impedance of the hand. Impedance methods have high impact over position and contact force control. The impedance problem is defined as proposing a single controller with estimated contact force exerted by the object on the robot hand that regulates motion trajectory and contact force with or without knowledge of

object stiffness. It was first introduced by Hogan [3]. The general impedance law is defined as,

$$F_d - F_c = M_I(\ddot{X}_d - \ddot{X}_r) + B_I(\dot{X}_d - \dot{X}_r) + K_I(X_d - X_r) \tag{32}$$

In (32), force error $e_f = F_d - F_c$ drives the mechanical impedance properties of the object where, X_r is the regulated object position trajectory driven by $e_f = F_d - F_c$. To calculate the resultant force exerted by object, substitute (32) into object dynamics of (10) yields,

$$F_o = (M_o - M_I)\ddot{e} + B_I\dot{e} + K_I e + C_o(X_o, \dot{X}_o) \tag{33}$$

The impedance error should tend to zero and can be expressed mathematically,

$$\lim_{t\to\infty} X_d - X_r \approx 0 \tag{34}$$

The resultant force found from (33) is to realize the desired coupled compliance of (32). The contact force F_c can be calculated from (11) as,

$$F_c = G^+ F_o + F_I \tag{35}$$

where, F_I is the internal force. Reference trajectory is then regulated from (33) for tracking control by HOSM. The integration of adaptation mainly focuses on generating desired trajectory online as a function of force tracking error e_f. When contact force is generated, the online based desired object trajectory is defined as,

$$X_d(t) = f(t) + k_p(t)e_F(t) + k_d(t)\dot{e}_F(t) \tag{36}$$

where, $f(t)$ is the auxiliary input, generated by the adaptation scheme. $k_p(t)$ and $k_v(t)$ are adaptive proportional gains driving force error and error rate. These are determined by the P-I adaptation laws below:

$$\begin{matrix} a(t) = a(0) + \alpha_1 \int_0^t q(t)dt + \alpha_2 q(t) \\ k_p(t) = k_p(0) + \beta_1 \int_0^t q(t)e_F(t)dt + \beta_2 q(t)e_F(t) \\ k_d(t) = k_d(0) + \gamma_1 \int_0^t q(t)\dot{e}_F(t)dt + \gamma_2 q(t)\dot{e}_F(t) \\ q(t) = w_p e_F(t) + w_d \dot{e}_F(t) \end{matrix} \tag{37}$$

where, w_p and w_d are weighting factors object position and velocity. The terms $(\alpha_1, \beta_1, \gamma_1)$ are integral adaptation gains, and $(\alpha_2, \beta_2, \gamma_2)$ are proportional adaptation gains. The online based trajectory X_d is calculated from (36) and (37) where $X_d(0) = a(0)$. This online based X_d is fed by the impedance filter (32) to extract regulated trajectory X_r. The regulated X_r is then tracked by HOSM control method. Two control methods applied to the multifingered hand is shown in Figure 2.

III. SIMULATION AND RESULTS

For the Barrett hand simulation, link lengths, $l_1 = 0.05m, l_2 = 0.07m, l_3 = 0.07m$, link mass, $m_1 = 0.03kg, m_2 = 0.05kg, m_3 = 0.03kg$, base height of the hand, $h = 0.05m$, gravity, $g = 9.81m/s^2$. The HOSM parameters before grasp: sliding constant, $\lambda = 0.04$, switching gain, $K_h = 18$, gain, $\alpha = 1.8$. After grasp, HOSM control parameters in object space are: Sliding constant, $\lambda = 0.01$, Switching gain, $K_h = 12$, gain, $\alpha_h = 1.1$. AFIM mode is dependent on the contact force. Desired force F_d is chosen as $10\,N$. Impedance parameters are $M_I = 23, B_I = 70$ and
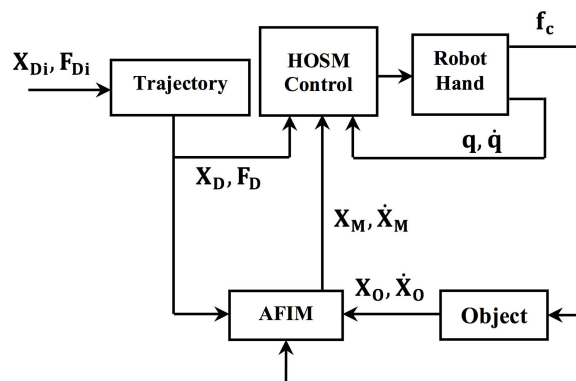
Figure 2. Proposed control architecture of HOSM-AFIM.

$K_I = 450$. The adaptive parameters are: k_p, k_d, w_p and w_d are selected as $1.4, 0.041, 0.02$ and 0.001 respectively.

At first, fingers are simulated in joint space to see the tracking performance with HOSM. Desired trajectories of the fingers are given for both mode as $[sp, q_2, q_3] = [0.7854, 0.6109, 0.4363]$ rad. In Figure 3 and 4, joint motion of fingers are compared between HOSM and general computed torque method (CTC). It appears that the overshoots are less and settling down is quick with HOSM considering uncertainties. Trajectories are well tracked with disturbances given as additional input into the system. In Figure 5, control torques of finger F_3 are shown with SMC (Top) and HOSM (Bottom). The input signal chattering is visible with SMC, common in first order sliding mode. The chatterings are completely eliminated with HOSM which indicates that HOSM is not only able to achieve precise tracking performance but also provides smooth torque to drive the joints. Then, the system is simulated to assess the performance of object manipulation after grasp. The object position and orientation errors are shown in Figure 6 and 7 respectively. The HOSM based manipulation errors are compared with CTC. The error are large with CTC method and not converging to zero for few motion vectors. The motion errors are improved and converged to zero with HOSM. Figure 8 shows the tracked normal contact forces of all fingers for desired force input of $10\ N$. The results are compared with natural impedance filter. The steady state errors are found with impedance law. Overshoots are reduced and steady state errors are minimized with AFIM mode.

IV. CONCLUSION

Two adaptive and robust control methods are proposed for grasping and manipulation of an object by multifingered robot hand. Sliding mode based HOSM control is proposed due to the high precision tracking requirements for performing manipulation tasks. Joint and object motion tracking results indicate the authenticity of the HOSM control algorithm. The AFIM process is efficient in generating a grasp of an object with a desired force estimated by object stiffness properties. Addition of adaptation helped to achieve the desired force. This method ensures not to cause any damage to the object as the fingers only exert the desired force to grasp and manipulate the object. Control objectives are successfully achieved by the proposed methods and the simulated results.
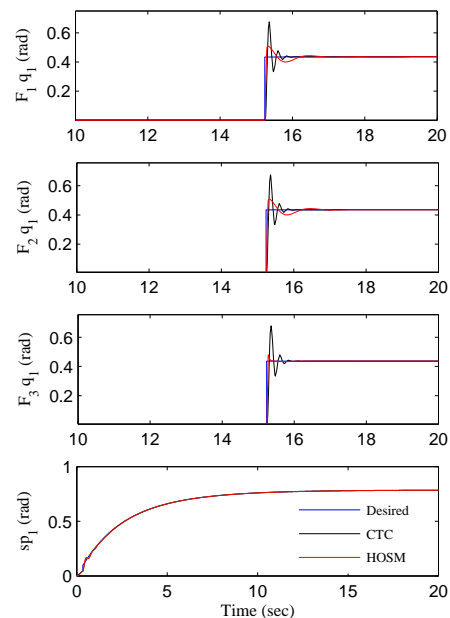
Figure 3. First revolute joint q_2 and sp_1 results of all fingers.
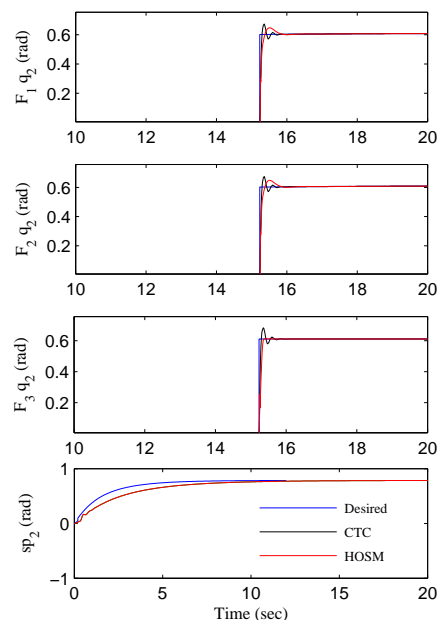
Figure 4. Second revolute joint q_3 and sp_2 results of all fingers.

REFERENCES

[1] S. Arimoto, R. Ozawa, and M. Yoshida, "Two-dimensional stable blind grasping under the gravity effect," in Robotics and Automation, 2005. ICRA 2005. Proceedings of the 2005 IEEE International Conference on. IEEE, 2005, pp. 1196–1202. [Online]. Available: http://ieeexplore.ieee.org/xpls/abs_all.jsp?arnumber=1570278

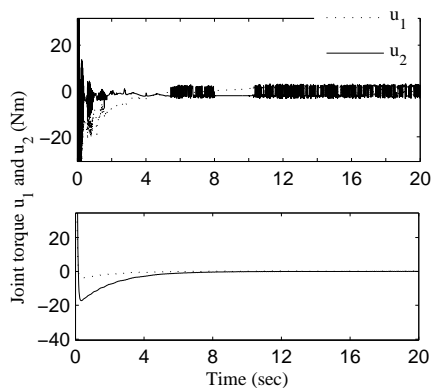[2] A. Bicchi and V. Kumar, "Robotic grasping and contact: A review," in ICRA. Citeseer, 2000, pp. 348–353.

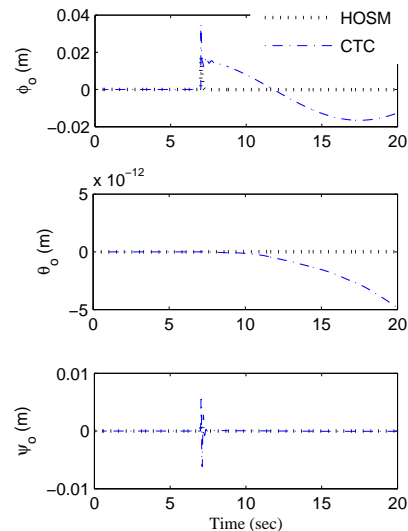Figure 5. Chattering elimination of joint torque τ with HOSM for finger F_3; SMC (Top) HOSM (Bottom).

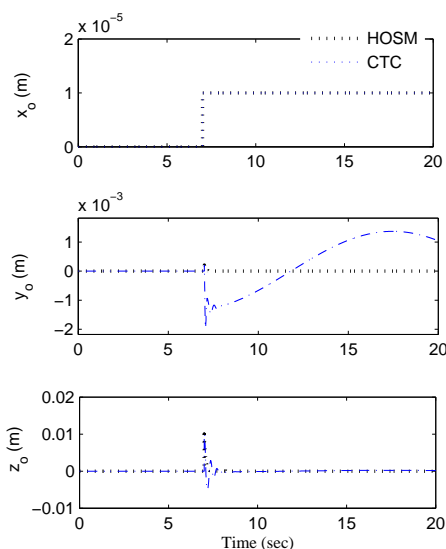Figure 6. Object position error comparison with HOSM and CTC law.

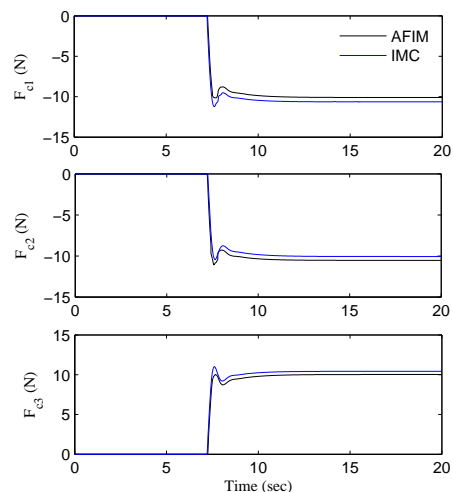Figure 7. Object orientation error comparison with HOSM and CTC law.

Figure 8. Contact force comparison with IMC and AFIM law.

[3] A. B. Cole, J. E. Hauser, and S. S. Sastry, "Kinematics and control of multifingered hands with rolling contact," Automatic Control, IEEE Transactions on, vol. 34, no. 4, 1989, pp. 398–404. [Online]. Available: http://ieeexplore.ieee.org/xpls/abs_all.jsp?arnumber=28014

[4] M. Defoort, T. Floquet, A. Kokosy, and W. Perruquetti, "A novel higher order sliding mode control scheme," Systems & Control Letters, vol. 58, no. 2, 2009, pp. 102–108. [Online]. Available: http://www.sciencedirect.com/science/article/pii/S0167691108001588

[5] F. Dinuzzo and A. Ferrara, "Higher order sliding mode controllers with optimal reaching," Automatic Control, IEEE Transactions on, vol. 54, no. 9, 2009, pp. 2126–2136. [Online]. Available: http://ieeexplore.ieee.org/xpls/abs_all.jsp?arnumber=5208186

[6] N. Hogan, "Impedance control: An approach to manipulation: Part itheory, part ii-implementation, part iii-applications," Journal of Dynamic Systems, Measurement, and Control, 1985, p. 1.

[7] S. Jung, T. C. Hsia, and R. G. Bonitz, "Force tracking impedance control for robot manipulators with an unknown environment: theory, simulation, and experiment," The International Journal of Robotics Research, vol. 20, no. 9, 2001, pp. 765–774. [Online]. Available: http://ijr.sagepub.com/content/20/9/765.short

[8] J. Kerr and B. Roth, "Analysis of multifingered hands," The International Journal of Robotics Research, vol. 4, no. 4, 1986, pp.

3–17. [Online]. Available: http://ijr.sagepub.com/content/4/4/3.short

[9] A. Levant, "Higher-order sliding modes, differentiation and output-feedback control," International Journal of control, vol. 76, no. 9-10, 2003, pp. 924–941. [Online]. Available: http://www.tandfonline.com/doi/abs/10.1080/0020717031000099029

[10] M. T. Mason and J. K. Salisbury Jr, Robot hands and the mechanics of manipulation. MIT press, 1985.

[11] T. Okada, "Computer control of multijointed finger system for precise object-handling," Systems, Man and Cybernetics, IEEE Transactions on, vol. 12, no. 3, 1982, pp. 289–299. [Online]. Available: http://ieeexplore.ieee.org/xpls/abs_all.jsp?arnumber=4308818

[12] A. M. Okamura, N. Smaby, and M. R. Cutkosky, "An overview of dexterous manipulation," in Robotics and Automation, 2000. Proceedings. ICRA'00. IEEE International Conference on, vol. 1. IEEE, 2000, pp. 255–262. [Online]. Available: http://ieeexplore.ieee.org/xpls/abs_all.jsp?arnumber=844067

[13] H. Seraji and R. Colbaugh, "Force tracking in impedance control," The

International Journal of Robotics Research, vol. 16, no. 1, 1997, pp. 97–117. [Online]. Available: http://ijr.sagepub.com/content/16/1/97.short

[14] C.-Y. Su and Y. Stepanenko, "Adaptive sliding mode coordinated control of multiple robot arms attached to a constrained object," Systems, Man and Cybernetics, IEEE Transactions on, vol. 25, no. 5, 1995, pp. 871–878. [Online]. Available: http://ieeexplore.ieee.org/xpls/abs_all.jsp?arnumber=376500

[15] W. Townsend, "The barretthand grasper–programmably flexible part handling and assembly," Industrial Robot: An International Journal, vol. 27, no. 3, 2000, pp. 181–188. [Online]. Available: http://www.emeraldinsight.com/journals.htm?articleid=875164&show=abstract

[16] T. Yoshikawa and K. Nagai, "Manipulating and grasping forces in manipulation by multifingered robot hands," Robotics and Automation, IEEE Transactions on, vol. 7, no. 1, 1991, pp. 67–77. [Online]. Available: http://ieeexplore.ieee.org/xpls/abs_all.jsp?arnumber=68071